MRS2015 / 6th International Workshop on Magnetic Resonance

Laterally constrained smooth and block inversion of quasi-two dimensional magnetic resonance tomography

Jiang Chuandong
College of Instrumentation & Electrical Engineering, Jilin University
Changchun, 130026, China
Chuandongjiang@gmail.com

Shang Xinlei
College of Instrumentation & Electrical Engineering, Jilin University
Changchun, 130026, China

Lin Tingting
College of Instrumentation & Electrical Engineering, Jilin University
Changchun, 130026, China

Fan Tiehu **Lin Jun**
College of Instrumentation & Electrical Engineering, Jilin University
Changchun, 130026, China

SUMMARY

We adapt a laterally constrained smooth and block inversion (LCSI and LCBI) scheme to increase the moderate and deep resolution of magnetic resonance tomography (MRT) for imaging quasi-two dimensional subsurface water-bearing structures. All the envelope data of the MRT signals from a profile are inverted together to produce the water content and relaxation time T_2^* distribution with vertical and lateral smooth transitions in the LCSI, while in the LCBI, the vertical thickness of the aquifer is also a solution with the lateral smooth transitions. Examples from synthetic 2D model and a field test show that the model reconstruction of a subsurface approximate layered aquifer is improved using LCSI and LCBI approach when compared with a combined 1D inversion and a 2D smooth inversion.

Key words: Laterally constrain, inversion, 2D, smooth, block

INTRODUCTION

Surface nuclear magnetic resonance (surface NMR) is a promising technique that provides direct quantitative information about the spatial location and amount of water in the subsurface (Legchenko et al., 2002). In many applications, surface NMR is used for one-dimensional (1D) depth sounding using a coincident transmitter and receiver loop and is referred to as magnetic resonance sounding (MRS). Recently, the application of surface NMR to 2D targets has been used to characterize laterally heterogeneous subsurface aquifer structures, such as buried glacial valleys, fractured bedrock, karst conduits and caverns, and it's commonly referred to as magnetic resonance tomography (MRT). Surface NMR including separated transmitter and receiver loops has been applied to enhance spatial resolution capabilities (Hertrich et al., 2009) at shallow depths. However, to the moderate and deep aquifer, the inversion resolution of 2D imaging is insufficient.

We apply the idea of the laterally constrained inversion (LCI; Auken et al., 2005) in order to increase the resolution of quasi-2D MRT when targeting moderate and deep water bearing structures. Although the LCI scheme has been successful used for quasi-2D and 2D resistivity imaging in electromagnetic method, it is rarely applied for a MRT investigation, only one reports the first attempt on joint inversion of MRS and TEM data (Behroozmand et al., 2012). Thus, we evaluate the resolution capabilities including the quasi-2D laterally constrained smooth and block inversion (LCSI and LCBI) in comparison to a traditional 1D smooth and block inversion using a 2D synthetic study and a field test. At last, we conduct a 2D smooth inversion of the MRT data to indicate the reason of low resolution and propose the feasible improvement method.

METHOD AND RESULTS

Quasi-2D model set-up

A quasi-2D model is a combination of laterally constrained 1D models along a profile as shown in Fig.1. The lateral distance between the models is controlled by the sampling density of the data and may be non-equidistant. For the LCSI, as the thickness is fixed, the layer parameters are water content w and relaxation time T_2^*, while for the LCBI, the thickness h is also variable. The parameters $R^w, R^{T_2^*}, R^h$ are the water content constraint, relaxation time constraint and thickness constraint, respectively, connected with the lateral layers between the neighbored models.

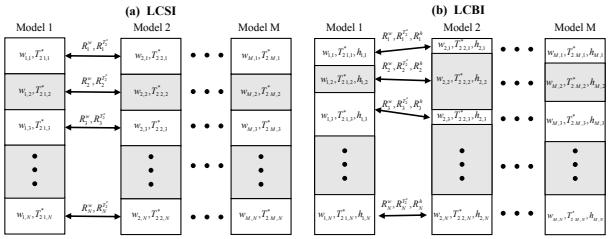

Figure 1. LCSI and LCBI model set-up

All the envelop data of the MRT signal is used for the forward modeling and inversion. The 1D forward expression is given by Hertrich et al. (2009),

$$V(q,t) = \int K(q,z) \cdot w(z) \cdot e^{-\frac{t}{T_2^*(z)}} dz \qquad (1)$$

where $V(q,t)$ is the measured envelop signal depending on pulse moment q and time t, $K(q,z)$ is the kernel function in detail described by Hertrich et al. (2009). To a profile, M MRT soundings with Q pulse moments and T sampling data are recorded. Assume there are N fixed-thickness layers in the subsurface in the smooth inversion, the forward expression is discretized as

$$\mathbf{V} = \mathbf{KW} \qquad (2)$$

where $\mathbf{V}=[\mathbf{V}_1;\mathbf{V}_2;\cdots \quad _M$ is a vertical vector with $\mathbf{V}_i=\begin{bmatrix} V_i(q_1,t_1),\cdots V_i\ q\ t_T), \\ V_i(q_2,t_1),\cdots V_i\ q\ t_T), \\ \cdots \\ V_i(q_Q,t_1),\cdots V_i\ q_Q\ t_T) \end{bmatrix}^{\mathrm{T}}$, $\mathbf{K}$=diag$[\mathbf{K}_1,\mathbf{K}_2,\cdots \quad _M$ is a matrix with $\mathbf{K}_i=\begin{bmatrix} K(q_1,z_1) & K(q_1,z_2) & \cdots & K\ q\ ,z_N) \\ K(q_2,z_1) & K(q_2,z_2) & \cdots & K\ q\ ,z_N) \\ \vdots & \vdots & \ddots & \vdots \\ K(q_Q,z_1) & K(q_Q,z_2) & \cdots & K\ q_Q,z_N) \end{bmatrix}$, and $\mathbf{W}=[\mathbf{W}_1;\mathbf{W}_2;\cdots \quad _M$ is a vertical vector with $\mathbf{W}_i=\begin{bmatrix} w_i(z_1)\mathrm{e}^{-\frac{t_1}{T_{2i}^*(z_1)}},\cdots w_i\ z_N)\mathrm{e}^{-\frac{t_1}{T_{2i}^*(z_N)}}, \\ w_i(z_1)\mathrm{e}^{-\frac{t_2}{T_{2i}^*(z_1)}},\cdots w_i\ z_N)\mathrm{e}^{-\frac{t_2}{T_{2i}^*(z_N)}}, \\ \cdots \\ w_i(z_1)\mathrm{e}^{-\frac{t_T}{T_{2i}^*(z_1)}},\cdots w_i\ z_N)\mathrm{e}^{-\frac{t_T}{T_{2i}^*(z_N)}} \end{bmatrix}^{\mathrm{T}}$.

Lateral Constrained Smooth Inversion

To image the quasi-2D water content and T_2^* distribution in the subsurface, we adapted the lateral constraint to the qt inversion (QTI) approach (Mueller-Petke and Yaramanci, 2010), the objective function Φ for the optimization problem is

$$\Phi=\left\|\mathbf{D}(\mathbf{V}-\mathbf{Gm})\right\|_2^2+\lambda\left\|\mathbf{Cm}\right\|_2^2\rightarrow\min \tag{3}$$

where $\mathbf{D}=\mathbf{1}/\boldsymbol{\varepsilon}_{\mathbf{d}}$ is the error estimate of the envelop data $\mathbf{V}$, $\mathbf{G}$ is the Jacobian matrix including the kernel function $\mathbf{K}$,

$$\mathbf{G}=\left[\mathbf{G}_w,\mathbf{G}_{T_2^*}\right] \tag{4}$$

with the j-layer in the i-model at the m-pulse moment and n-time sample

$$\frac{\partial V(q_m,t_n)}{\partial w_i(z_j)}=K(q_m,z_j)\cdot e^{-\frac{t_n}{T_{2i}^*(z_j)}}$$

$$\frac{\partial V(q_m,t_n)}{\partial T_{2i}^*(z_j)}=\frac{t_n}{T_{2i}^*(z_j)^2}\cdot K(q_m,z_j)\cdot w_i(z_j)\cdot e^{-\frac{t_n}{T_{2i}^*(z_j)}}.$$

$\mathbf{m}=\left[\mathbf{w},\mathbf{T}_2^*\right]$ is the desired solution and $\mathbf{C}$ is the first-order flatness matrix that including the vertical and lateral smooth constraints C_V and C_R

$$\mathbf{C}=\begin{bmatrix}\mathbf{C}_w & 0\\ 0 & \mathbf{C}_{T_2^*}\end{bmatrix} \tag{5}$$

where $\mathbf{C}_{w|T_2^*}=\begin{bmatrix}C_{V_{w|T_2^*}}\\ C_{R_{w|T_2^*}}\end{bmatrix}=\left[\begin{array}{cccccccc} -1 & 1 & 0 & 0 & \cdots & \cdots & & 0 \\ 0 & -1 & 1 & 0 & \cdots & \cdots & & 0 \\ \vdots & \vdots & \vdots & \vdots & \ddots & \ddots & \vdots & \vdots \\ 0 & 0 & 0 & 0 & \cdots & \cdots & & 1 \\ \hline -1 & 0 & \cdots & & & & \cdots & \\ 0 & -1 & 0 & \cdots & & & & \cdots \\ \vdots & \vdots & \ddots & \ddots & \ddots & \ddots & \ddots & \vdots \\ 0 & 0 & \cdots & & & \cdots & & \end{array}\right]$.

The complex kernels $\mathbf{G}$ are transferred to $\mathbf{J}=f^{A,tan}(\mathbf{G})$ delivering amplitude data, and the subsurface water content w and T_2^* is restricted to a geologically-meaningful range (0-100% and 0-1000 ms) using a tangent transform. We use a conjugate gradient solver to derive the model update $\Delta\mathbf{m}_k$ in each iteration step k by solving the regularized normal equation

$$\left(\mathbf{J}^{\mathrm{T}}\mathbf{D}^{\mathrm{T}}\mathbf{DJ}+\lambda\mathbf{C}^{\mathrm{T}}\mathbf{C}\right)\Delta\mathbf{m}_k=\mathbf{J}^{\mathrm{T}}\mathbf{D}^{\mathrm{T}}\mathbf{D}\Delta\mathbf{d}_k-\lambda\mathbf{C}^{\mathrm{T}}\mathbf{Cm}_k \tag{6}$$

where $\Delta\mathbf{d}_k=\mathbf{d}-\mathbf{Jm}_k$ contains the misfit between the observed and estimated data. In addition, an explicit line search procedure is applied to optimize the step length.

Lateral Constrained Block Inversion

The block inversion is based on the assumption that subsurface can be represented by a small number of discrete boundaries. Assuming that three layers with water content $w=[w_1,w_2,w_3]$, relaxation time $T_2^*=\left[T_{21}^*,T_{22}^*,T_{23}^*\right]$ and thickness $h=[h_1,h_2,h_3]$ are sufficient, the forward expression (1) can be rewritten as

$$\begin{aligned} V(q,t)=&\int_0^{h_1}K(q,z)\cdot w_1\cdot e^{-\frac{t}{T_{21}^*}}dz\\ &+\int_{h_1}^{h_1+h_2}K(q,z)\cdot w_2\cdot e^{-\frac{t}{T_{22}^*}}dz\\ &+\int_{h_1+h_2}^{h_1+h_2+h_3}K(q,z)\cdot w_3\cdot e^{-\frac{t}{T_{23}^*}}dz \end{aligned} \tag{7}$$

The Jacobian matrix of this forward operator in respect to w, T_2^*, h is given by

$$\mathbf{G}=\left[\mathbf{G}_w,\mathbf{G}_{T_2^*},\mathbf{G}_h\right] \tag{8}$$

with

$$\frac{\partial V(q_m,t_n)}{\partial w_{i,1\text{-}3}}=\begin{bmatrix}\int_0^{h_1}K(q_m,z)\cdot e^{-\frac{t_n}{T_{2i,1}^*}}dz,\\ \int_{h_1}^{h_1+h_2}K(q_m,z)\cdot e^{-\frac{t_n}{T_{2i,2}^*}}dz,\\ \int_{h_1+h_2}^{h_1+h_2+h_3}K(q_m,z)\cdot e^{-\frac{t_n}{T_{2i,3}^*}}dz\end{bmatrix}=\left[K1_m\cdot e^{-\frac{t_n}{T_{2i,1}^*}},K2_m\cdot e^{-\frac{t_n}{T_{2i,2}^*}},K3_m\cdot e^{-\frac{t_n}{T_{2i,3}^*}}\right]$$

$$\frac{\partial V(q_m,t_n)}{\partial T_{2i,1\text{-}3}^*}=\left[\frac{t_n}{T_{2i,1}^{*2}}\cdot K1_m\cdot w_{i,1}\cdot e^{-\frac{t_n}{T_{2i,1}^*}},\frac{t_n}{T_{2i,2}^{*2}}\cdot K2_m\cdot w_{i,2}\cdot e^{-\frac{t_n}{T_{2i,2}^*}},\frac{t_n}{T_{2i,3}^{*2}}\cdot K3_m\cdot w_{i,3}\cdot e^{-\frac{t_n}{T_{2i,3}^*}}\right]$$

$$\frac{\partial V(q_m,t_n)}{\partial h_{i,1\text{-}2}}=\begin{bmatrix}\left(\frac{t_n}{T_{2i,2}^{*2}}\cdot w_{i,2}\cdot e^{-\frac{t_n}{T_{2i,2}^*}}-\frac{t_n}{T_{2i,1}^{*2}}\cdot w_{i,1}\cdot e^{-\frac{t_n}{T_{2i,1}^*}}\right)K(q_m,h_1)\\ +\left(\frac{t_n}{T_{2i,3}^{*2}}\cdot w_{i,3}\cdot e^{-\frac{t_n}{T_{2i,3}^*}}-\frac{t_n}{T_{2i,2}^{*2}}\cdot w_{i,2}\cdot e^{-\frac{t_n}{T_{2i,2}^*}}\right)K(q_m,h_1+h_2),\\ \left(\frac{t_n}{T_{2i,3}^{*2}}\cdot w_{i,3}\cdot e^{-\frac{t_n}{T_{2i,3}^*}}-\frac{t_n}{T_{2i,2}^{*2}}\cdot w_{i,2}\cdot e^{-\frac{t_n}{T_{2i,2}^*}}\right)K(q_m,h_1+h_2)\end{bmatrix}.$$

Then the solution is $\mathbf{m}=\left[\mathbf{w},\mathbf{T}_2^*,\mathbf{h}\right]$ and the smooth matrix is

$$\mathbf{C}=\begin{bmatrix}\mathbf{C}_w & 0 & 0\\ 0 & \mathbf{C}_{T_2^*} & 0\\ 0 & 0 & \mathbf{C}_h\end{bmatrix}. \tag{6}$$

Synthetic Example

The synthetic data (see Fig. 2) are calculated using a 2D MRT kernel function described by Hertrich et al. (2009). The square loop with a 100-m loop side is layout on ten positions (P1-P10) by edge to edge, to cover a 1000-m profile. The earth's magnetic field is set to 54,720 nT at an inclination of 60º and a declination of 0º. The resistivity in the subsurface of the whole profile is 100 Ωm. The water-bearing model chosen

from a common structure consists of three part: 1) shallow and thick aquifer; 2) medium depth and thin aquifer; and 3) deep and thick aquifer (see Fig. 2a&b). The three parts are laterally connected to a whole aquifer. The water content and the relaxation time T_2^* of the aquifer is 40%, and 400 ms, and the other space is 1% and 100 ms, meaning a gravel aquifer inside a dry sand. To show the superiority of the results from LCI, a very high noise level with a standard deviation of 1,000 nV (before gating) is added to the MRS signals. After gating, the noise-to-signal ratio (SNR) is still very low, especially in the positions P5-P10, i.e. over the thin aquifer and the deep aquifer (see Fig. 2c).

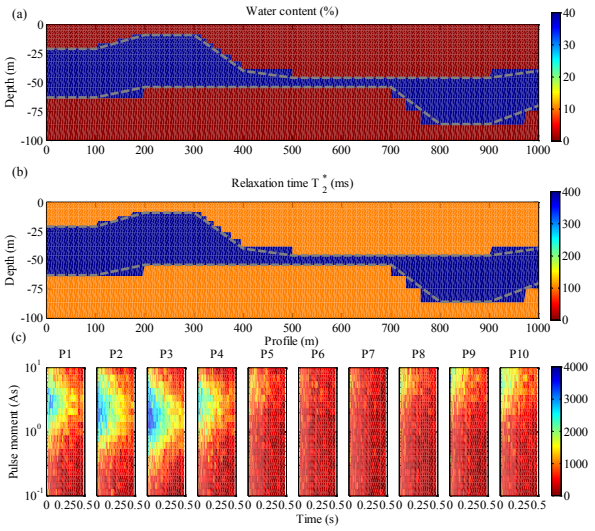

Figure 2. Synthetic model of 2D MRT

The results of 1D smooth inversion and quasi-2D LCSI are shown in Figure 3. For the 1D smooth inversion, ten results are pieced together to a profile (Fig. 3a&c). As the aquifer is shallow and thick and the SNR of data is high, the water content is basically correct in the positions P1-P5, only not continuous in the lateral. However, the thin aquifer (P6-P7) in the medium depth is missing, and the deep thick aquifer (P8-P10) is very blurry, only the upper boundary is visible. For the relaxation time T_2^*, the image is so confused that cannot find out the aquifer. On contrast, although the SNR is very low, the shape of the aquifer from quasi-2D LCSI (Fig. 3b&d) is clear, and the water content is close to 40% in the whole aquifer because of the lateral constraint. The thin aquifer and the deep aquifer are both reconstructed well, only a little gradually varying on the bottom of the deep aquifer due to the low resolution here. In addition, a thin aquifer on the top of the surface appears mainly because of the low SNR. The result of the relaxation time T_2^* is also much better than 1D smooth inversion. The shape is a little wider than the model, because the water content outside the aquifer is low, resulting a low resolution on the T_2^*. Beside the shallow thin aquifer on the surface, the main aquifer is inverted well.

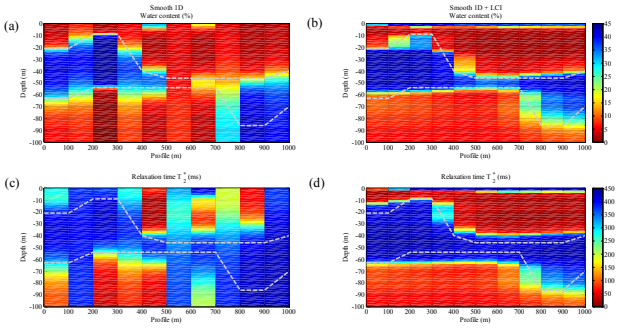

Figure 3: Water content and T_2^* results from 1D smooth inversion and quasi-2D smooth-LCI

Figure 4 shows the results of 1D block inversion and quasi-2D LCBI. The images are similar to these in the Fig. 3. The block number is set to 4 in each position. The shallow aquifer is reconstructed correctly by both of the inversion methods. However, the thin aquifer and deep aquifer from quasi-2D LCBI are much better than those from 1D block inversion. Contrast with the smooth inversion, the upper and bottom boundaries of the aquifer are much apparent, and there is not the fake thin aquifer on the surface. The only disadvantage of quasi-2D LCBI is the composition of two aquifers (e.g. P1-P2) with small different thickness, because of the strong lateral constraint. Moreover, the results of relaxation time T_2^* also demonstrate the quasi-2D LCBI method is much clearly on the boundaries of the aquifer than the quasi-2D LCSI method.

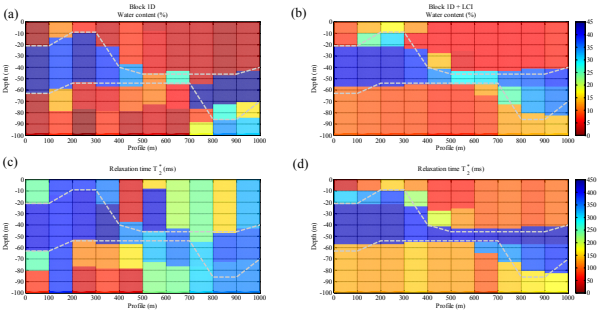

Figure 4. Water content and T_2^* results from 1D block inversion and quasi-2D block-LCI

Field test

A field test for a quasi-2D MRT data set was carried out in Iwatara Basin, Mongolia, in the winter of 2009. Field measurements are carried out with a Tx/Rx coincident square loop of 100-m-side for the maximum detection depth of 100 m. Earth magnetic field is measured by a magnetometer and corresponded to the Larmor frequency is in the range of 2460 to 2482 Hz. The ambient noise level measured is between 140 and 300 nV, only occasionally over 1000 nV. During the MRS measuring, 16 exciting pulses of increasing energy with 40 ms duration time are used. During this survey the standard SAMOVAR software (IRIS Instruments, 2006) based on the Tikhonov regularization method is used for comparing with MRT profile results in quasi-2D (Figure 5).

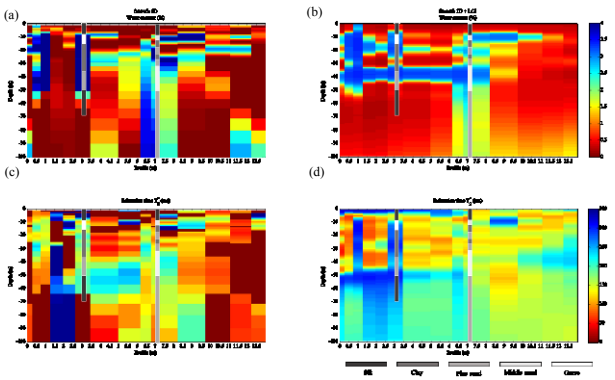

Figure 5: Water content and T_2^* results from 1D smooth inversion and quasi-2D LCSI in field test

The results of water content and relaxation time T_2^* from 1D smooth inversion are complicated. Although the borehole logging results are consistent with the partial site, we cannot divide the whole profile by multiple aquifers. On contrast, the quasi-2D LCSI results are more recognizable on the aquifers, and also comparable with the borehole log. However, due to various distances and surface altitudes, these results need further improving and other geophysical results as the priori information.

Discuss and Outlook

Quasi-2D image cannot be instead of a true 2D image, which is inverted with the 2D kernel function. However, the results from the 2D smooth inversion (Fig. 6) is unsufficient good either. This is mainly because of the loop layout (edge-to-edge), which can provide a relatively low resolution in the medium and deep depth, as well as the high noise level. In the 2D smooth inversion, there is a flatness matrix to constrain the vertical and lateral direction, but the constraint range is small and weak, only effects on the direct neighbors. On the other hand, the model is approximate layered, thus on every position, the results can be inverted by 1D inversion. Therefore, the quasi-2D image is more suitable for this model. Furthermore, if a more non-layered model, the 2D inversion may provide more details about the water-bearing structure, but need improve the resolution and accuracy. A block and laterally constrained 2D inversion method demands further research.

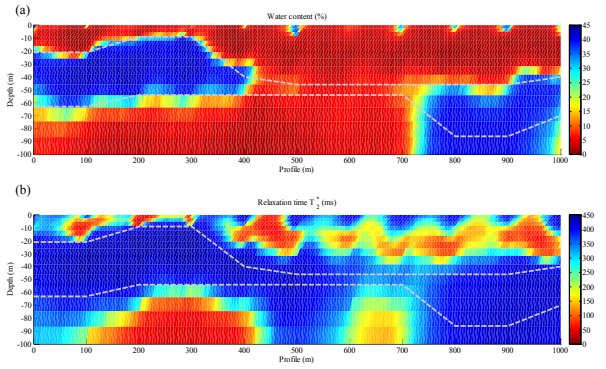

Figure 6: Water content and T_2^* results from 2D smooth inversion

CONCLUSIONS

In this paper, a laterally constrained smooth and block inversion scheme (LCSI and LCBI) is proposed and evaluated in the quasi-2D MRT for imaging subsurface water-bearing structures. Firstly, based on the envelop data of the MRT signal, we derived the inversion iterative equation with Jacobian matrix in respect to the water content and relaxation time T_2^* in the LCSI method, and additional the thickness in the LCBI method, as well as the flatness matrix with vertical and lateral constraint. Secondly, we evaluate the quasi-2D LCSI and LCBI together with the traditional 1D smooth and block inversion using a synthetic 2D model, which shows the model reconstruction of the subsurface moderate and deep aquifer is much improved using LCSI and LCBI. At last, we indicate the results from the 2D smooth inversion are not as good as the quasi-2D LCI, but it can be improved by increasing the resolution or using a 2D block and LCI method instead.

REFERENCES

Auken, E., Christiansen, A. V., Jacobsen, B. H., et al, 2005, Piecewise 1D laterally constrained inversion of resistivity data: GEOPHYSICAL PROSPECTING, **53**, no. 4, 497-506.

Behroozmand, A. A., Auken, E., Fiandaca, G., et al, 2012, Improvement in MRS parameter estimation by joint and laterally constrained inversion of MRS and TEM data: GEOPHYSICS, **77**, no. 4, WB191-WB200.

Hertrich, M., Green, A. G., Braun, M., & Yaramanci, U., 2009, High-resolution surface-NMR tomography of shallow aquifers based on multi-offset measurements: GEOPHYSICS, **74**, no. 6, G47–G59.

Legchenko, A. & Valla, P., 2002, A review of the basic principles for proton magnetic resonance sounding measurements: JOURNAL OF APPLIED GEOPHYSICS, **50**, no. 1-2, 3–19.

Mueller-Petke, M. & Yaramanci, U., 2010, QT inversion — Comprehensive use of the complete surface NMR data set: GEOPHYSICS, **75,** no.4, WA199–WA209.